Available online at www.sciencedirect.com
ScienceDirect
Journal of the European Ceramic Society 29 (2009) 3099–3103
www.elsevier.com/locate/jeurceramsoc

Technical note

Structure and multiferroic properties of $BiFeO_3$ powders

De-Chang Jia*, Jia-Huan Xu, Hua Ke, Wen Wang, Yu Zhou

Institute for Advanced Ceramics, School of Materials Science and Engineering, Harbin Institute of Technology, Harbin 150001, China

Received 20 December 2008; received in revised form 7 April 2009; accepted 16 April 2009
Available online 17 May 2009

Abstract

Bismuth ferrite powders were synthesized by a simple sol–gel method at the temperature as low as 450 °C. Single phase $BiFeO_3$ powders with a rhombohedral perovskite structure were fabricated after Bi–Fe gels were calcined at 450–650 °C. Atomic ratio of Bi to Fe is approximately 1:1 for $BiFeO_3$ powders, as determined by energy dispersive X-ray spectrometer. $BiFeO_3$ powders show weak ferromagnetism at room temperature and strong size-dependent magnetic properties, which is different from the linear *M–H* relationship in $BiFeO_3$ ceramics. Dielectric anomaly at round 330 °C near the magnetic transition point corresponds to the antiferromagnetic to paramagnetic phase transition, indicating the coupling between polarization and magnetization in $BiFeO_3$ powders. A reversible ferroelectric phase transformation of $BiFeO_3$ powders has been detected at 827 °C by a differential thermal analysis.

Keywords: A. Calcinations; C. Dielectric properties; C. Magnetic properties; D. $BiFeO_3$

1. Introduction

$BiFeO_3$ is an attractive material because of its multiferroic properties, i.e., ferroelectricity with high Curie temperature (T_C = 820–850 °C[1,2]) and antiferromagnetic properties below Néel temperature (T_N = 350–380 °C[3,4]). $BiFeO_3$ shows antiferromagnetic G-type spin configuration along the $[1\,1\,1]_c$ or $[0\,0\,1]_h$ directions in its pseudocubic or rhombohedral structure. $BiFeO_3$ has a superimposed incommensurate cycloid spin structure with a periodicity of 620 Å along the $[1\,1\,0]_h$ axis at room temperature. This structure cancels the macroscopic magnetization and inhibits observation of the linear ME effect.[5,6] The decrease in particle size has been proved to be effective in suppressing this cycloid structure and enhancing the magnetic moment of $BiFeO_3$.[7,8] Interestingly, this ferromagnetic $BiFeO_3$ exhibits characteristic features in dielectric properties around the magnetic transition temperature, highlighting useful multiferroic behavior.[8] One of the main obstacles for $BiFeO_3$ applications is large leakage current because of the existence of the second phase, such as $Bi_2Fe_4O_9$, $Bi_{25}FeO_{40}$, and $Bi_{36}Fe_{24}O_{57}$.[8,9,11] Several attempts were done to obtain pure-phase $BiFeO_3$, such as sol–gel method,[11] precipitation/coprecipitation,[12] hydrothermal synthesis,[13] high energy ball milling[14] and the liquid phase sintering with a high heating rate (100 °C/s).[15] A solid solution system between $BiFeO_3$ and a ferroelectric material such as $PbTiO_3$,[16] $SrBi_2Nb_2O_9$[17,18] was also widely investigated.

In spite of these preparation techniques for pure $BiFeO_3$, studies on the phase structure, microstructure, relations between ferromagnetic properties and particle size of the $BiFeO_3$ prepared by a sol–gel method, are still rare in the literatures.

In this study, high purity as well as homogeneous nanoscale $BiFeO_3$ R-phase powders were obtained by a simple sol–gel method. The microstructure and magnetic properties of $BiFeO_3$ powders were investigated. Mulitiferrotic couple was determined by the dielectric anomaly near the magnetic transition point. Ferroelectric transition was detected by differential thermal analysis.

2. Experimental procedure

$BiFeO_3$ powders were synthesized by a simple sol–gel route. Details of powders preparation are available in our previous work.[19] The xerogel was calcined at various temperatures (450–700 °C) for 1 h in air for further characterization.

Crystal structures of $BiFeO_3$ powders were investigated by X-ray diffraction (XRD, Rigaku D/Max 2200VPC) with Cu Kα (λ = 1.5406 Å) radiation. The crystallite sizes (d_{XRD}) were

* Corresponding author. Tel.: +86 451 86418792; fax: +86 451 86418792.
E-mail address: dcjia@hit.edu.cn (D.-C. Jia).

0955-2219/$ – see front matter © 2009 Elsevier Ltd. All rights reserved.
doi:10.1016/j.jeurceramsoc.2009.04.023

calculated from X-ray peak broadening by Debye–Scherrer equation using the full width at half maximum (FWHM) data. De-conglomerated $BiFeO_3$ powders were transferred onto aluminum foil and coated with a thin Au coating for scanning electron microscope (SEM, Hitachi S-4700). Energy dispersive X-ray spectrometer (EDS, Horiba EMAX) was used to semi-quantitatively analyze the chemical composition of the synthesized powders. EX-350 software was used to analyze the obtained results. A drop of dilute suspension was dried on a carbon-coated microgrid for the transmission electron microscopy (TEM, Philips CM-12) observation. The room temperature magnetic properties were measured using a vibrating sample magnetometer (VSM, LakeShore M-7407). Differential thermal analysis (DTA, Netzsch, STA 449C Jupiter) was used to characterize the ferroelectric phase transition of $BiFeO_3$ powders in argon atmosphere. $BiFeO_3$ powders in alumina crucibles were heated to 880 °C at a rate of 10 °C/min, held for 1 h at 880 °C, and then cooled to ambient temperature at a rate of 10 °C/min. For the electrical measurement, $BiFeO_3$ powders calcined at 500 °C were cold isostatically pressed into a pellet with a diameter of 10 mm and a thickness of 1 mm under a pressure of 280 MPa, and then "sintered" at 500 °C for 10 h in air. The polished pellet with a silver paint was used for measuring temperature dependent dielectric property using a computer controlled HP4284 impedance analyzer.

3. Results and discussion

Fig. 1 shows the XRD patterns of $BiFeO_3$ powders calcined at different temperatures for 1 h. As it indicated, powders were rhombohedrally distorted perovskite structure. No impurity phases were detected in the powders calcined between 450 and 650 °C. Minor $Bi_2Fe_4O_9$ was detected in samples calcined at 700 °C, which is attributed to the decomposition of $BiFeO_3$ phase at high temperature.[9] It has been reported that a second-phase compound, $Bi_2Fe_4O_9$, formed above 675 °C.[10] The crystallite sizes of powders calcined at 450, 500, 550, 600, 650 and 700 °C for 1 h were noted to be about 26, 37, 55, 75, 102, 120 nm, respectively. The particle sizes could be estimated from SEM image as well as directly from TEM photographs. Figs. 2 and 3 show typical morphology of particle agglomerates. The particle size is slightly greater than the crystallite size obtained by the Scherrer equation because of agglomeration of the particles.

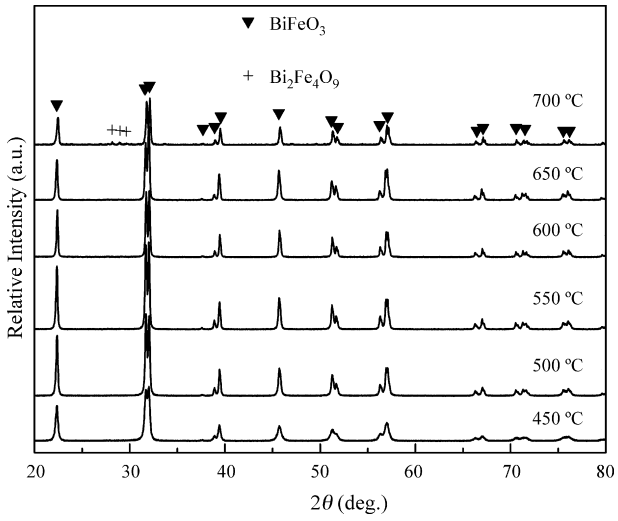

Fig. 1. XRD patterns of $BiFeO_3$ powders calcined at various temperatures.

Scanning electron microscopy (SEM) images of $BiFeO_3$ powders calcined at different temperatures are displayed in Fig. 2. It is clear that average particle size increases with the increase of thermal treatment temperature. SEM images of powders calcined at 500 and 600 °C show a relatively uniform grain size distribution, indicating it is a good method for sol–gel process to prepare powders with uniform features. The powders calcined at 700 °C exhibit a relatively regular shape and an inhomogeneous size distribution due to the crystallite growth at high temperature. Energy dispersive spectroscopy (EDS) analysis (Fig. 2(d)) shows that the atomic ratio of Bi to Fe is approximately 1:1 within the instrumental accuracy. TEM image of $BiFeO_3$ powders calcined at 600 °C for 1 h and corresponding selected area electron diffraction pattern (SAED) are shown in Fig. 3. The SAED pattern taken along the $[\bar{1}\,1\,0]$ zone axis from an individual particles shows sharp diffraction spots, indicating that $BiFeO_3$ particle is rhombohedrally distorted perovskite structure, which is consistent with the above XRD results. Moreover, the SAED patterns taken from different positions are found to be almost identical so that $BiFeO_3$ powders are well crystallized with a single-phase perovskite structure.

Fig. 4(a) shows the room temperature magnetization hysteresis loops for $BiFeO_3$ powders calcined at 500 °C. The partly enlarged *M–H* curve, shown in the inset of Fig. 4(a), exhibits a nonlinearity with the remanent magnetization of 0.004 emu/g and coercive field of 145 Oe, confirming the weak ferromagnetism nature at room temperature. In fact, $BiFeO_3$ is known to show a G-type antiferromagnetic ordering, but has a residual magnetic moment caused by its canted spin structure (weak ferromagnetism). The weak ferromagnetic order itself can be understood as a result of noncolinear (canted) spin arrangements in two sublattices.[20] Fig. 4(b) shows *M–H* curves of $BiFeO_3$ powders calcined at various temperatures for 1 h. $BiFeO_3$ powders exhibit the significant size effect. Saturation magnetization (M_s) decreases with the increase in particle size. Room temperature weak ferromagnetism in $BiFeO_3$ powders which is completely different from the linear *M–H* relationship in $BiFeO_3$ ceramics[21,22] should be attributed to size effect. Surface-volume ratio becomes large with decreasing particle size, the long-range antiferromagnetic order is frequently interrupted at the particle surfaces. The contribution of uncompensated spins at the surface to the total magnetic moment of the particle increases. Intrinsic spiral spin structure (period length of ~62 nm) is partially suppressed. In addition, surface anisotropies dominate magnetic behavior in small particles. Strain anisotropies at the surface possibly lead to the observed weak magnetization.[7] It is observed that the magnetization hysteresis loop of the sample calcined at 700 °C is almost similar to that of the sample calcined at 600 °C. This could be attributed to the magnetic contribution of the impurity phase exist in the samples calcined at 700 °C.

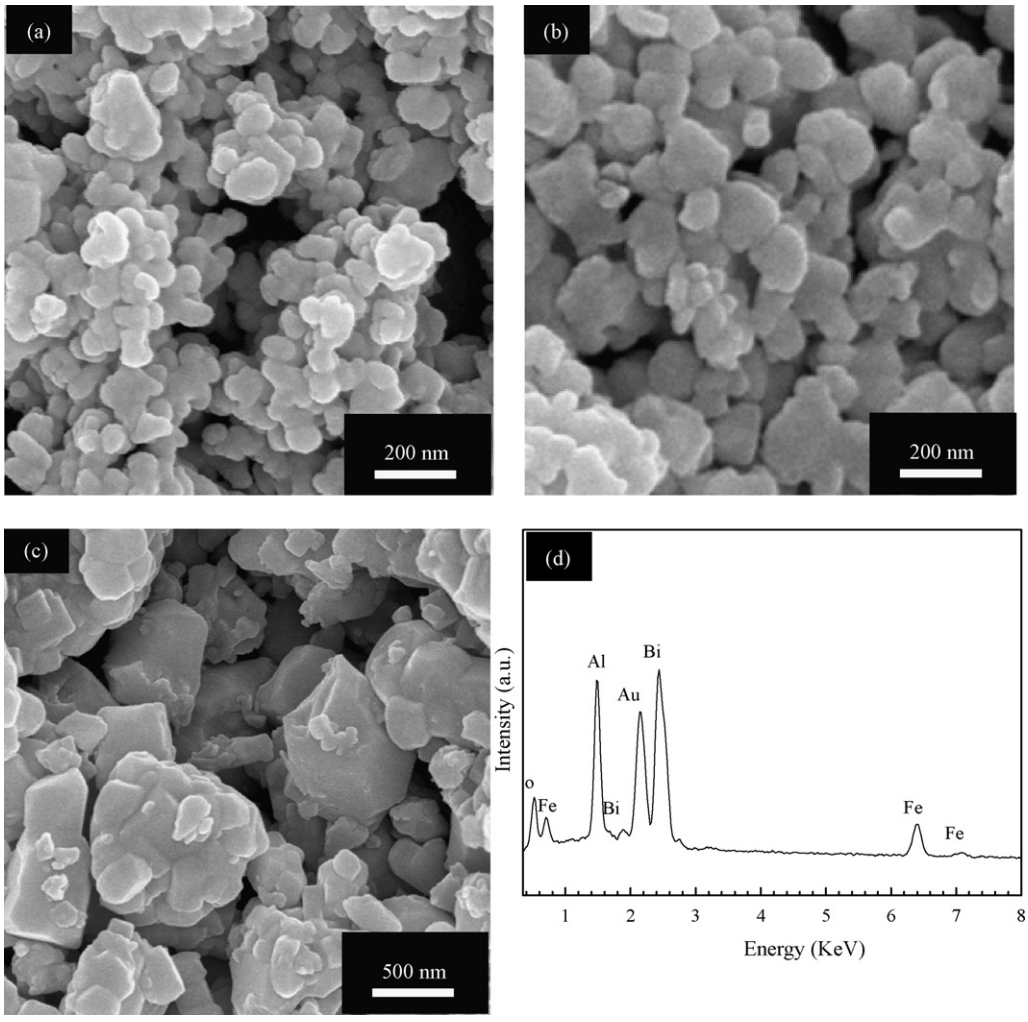

Fig. 2. SEM images of the $BiFeO_3$ powders calcined at: (a) 500 °C, (b) 600 °C, and (c) 700 °C. (d) EDS of $BiFeO_3$ powders calcined at 500 °C.

Fig. 5 shows the temperature dependence of the real part of the dielectric constant (ε') and dissipation factor (tan δ) for $BiFeO_3$ powders. A very abnormal diffuse dielectric pattern, containing an extremely high dielectric constant peak (on the order of 10^3), is observed in the ε'–T curve around 330 °C at 10 kHz during the heating process. The maximum of dielectric constant shifts toward higher temperature with increasing measurement frequency, reflecting a typical dielectric relax-

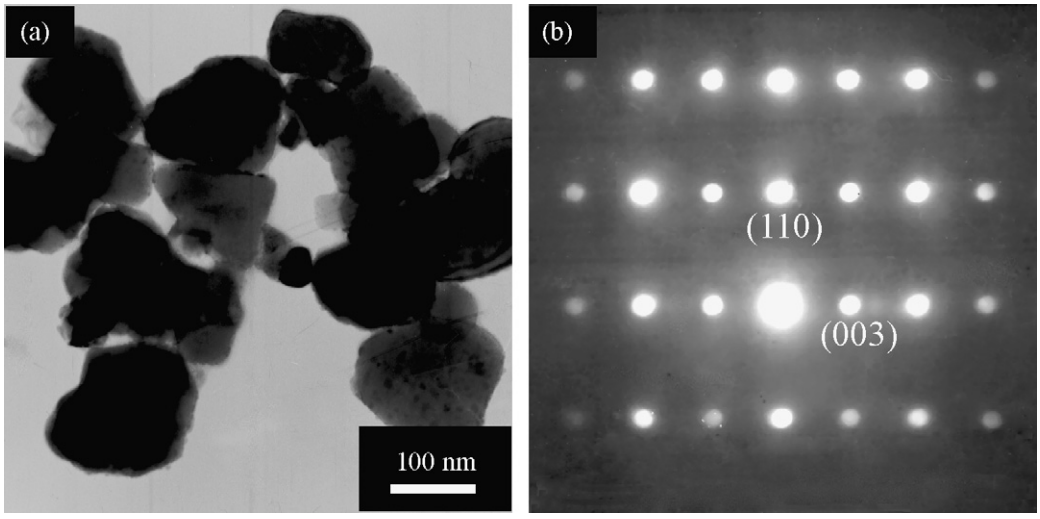

Fig. 3. TEM image of $BiFeO_3$ powders calcined at 600 °C (a) and its corresponding SAED pattern (b).

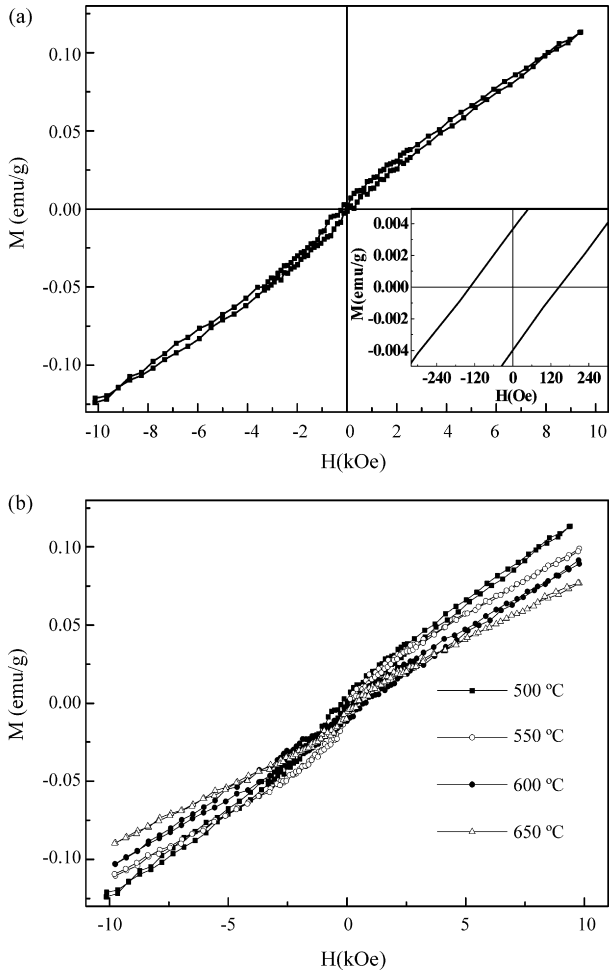

Fig. 4. Magnetic property of $BiFeO_3$ powders measured at room temperature: (a) *M–H* curve of $BiFeO_3$ powders calcined at 500 °C for 1 h, and (b) *M–H* curves of $BiFeO_3$ powders calcined at various temperatures for 1 h.

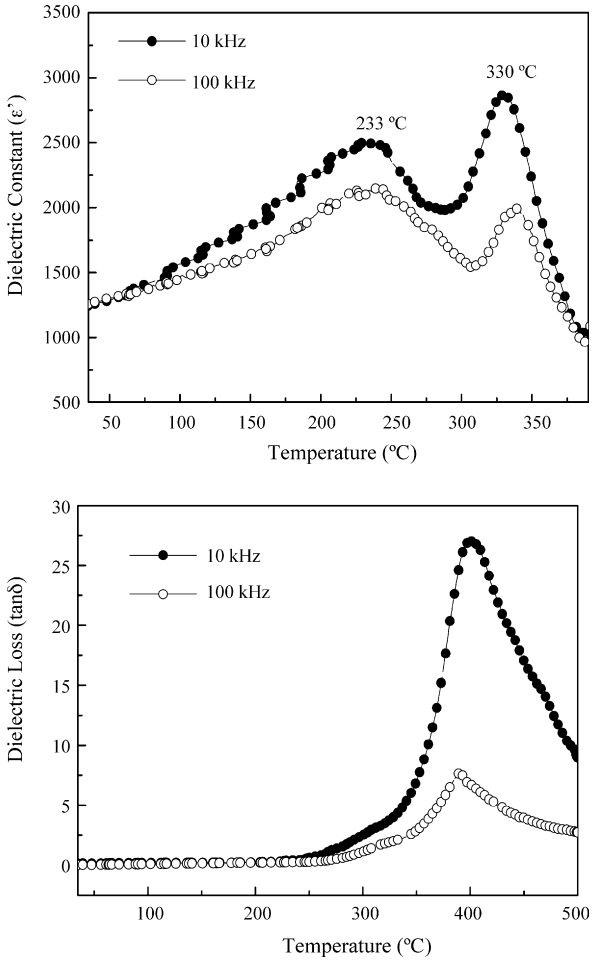

Fig. 5. Temperature dependence of the real part of dielectric constant (ε') and dissipation factor (tan δ) for $BiFeO_3$ powders measured at 10 and 100 kHz.

ation behavior. The anomaly at around 330 °C corresponds to the antiferromagnetic to paramagnetic phase transition at Néel temperature.[3,4] This phase transition is more clearly observed on an abnormal peak of dissipation factor (tan δ) versus temperature. The dielectric anomaly may signify coupling between polarization and magnetization, as expected in any multiferroic system such as $BiFeO_3$.[8] A dielectric anomaly around 230 °C is also observed, which seems to agree with the dielectric measurements in literatures.[16,23] The origin of this anomaly is needed to further study. In addition, great values of dissipation factors were due to the high leakage current in the $BiFeO_3$ pellet which is not dense enough.

To ascertain the ferroelectric nature of $BiFeO_3$ perovskite phase, $BiFeO_3$ powders calcined at 600 °C has been investigated by differential thermal analysis (DTA) while heating and cooling with heating/cooling rate of 10 °C/min in Ar atmosphere (Fig. 6). The endothermic and exothermic peaks were observed at 827 °C during heating and 813 °C during cooling, respectively. This indicates that ferroelectric phase transformation of $BiFeO_3$ powders is reversible. The observed thermal properties of $BiFeO_3$ powders are similar to those of $BiFeO_3$ ceramics prepared by sintering coprecipitated powder[12] and exactly coincide with those observed in hydrothermal synthesized $BiFeO_3$ crystallites.[24] The value of ferroelectric transition temperature obtained by DTA, however, slightly dependent on the processing conditions[12] and heating rate during measurement process.

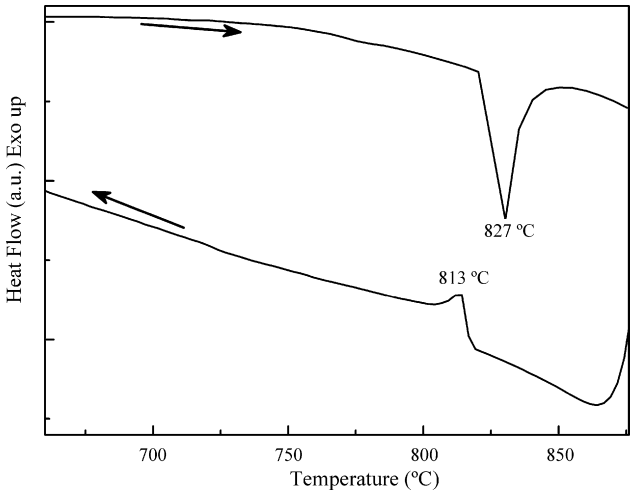

Fig. 6. DTA curves for $BiFeO_3$ powders calcined at 600 °C.

4. Conclusions

High purity $BiFeO_3$ R-phase powders have been successfully synthesized by a simple sol–gel process at a temperature as low as 450 °C. $BiFeO_3$ powders show room temperature weak ferromagnetism, which is completely different from room temperature magnetic properties of $BiFeO_3$ ceramics. Dielectric behavior of the $BiFeO_3$ powders is considered to the coupling of electric and magnetic order parameters. The ferroelectric transition temperature of $BiFeO_3$ was detected to be around 827 °C.

Acknowledgments

The authors thank the financial support by the Program of Excellent Teams in Harbin Institute of Technology (HIT) and Science Foundation for Distinguished Young Scholars of Heilongjiang Province.

References

1. Michel, C., Moreau, J. M., Achenbach, G. D., Gerson, R. and James, W. J., The atomic structure of $BiFeO_3$. *Solid State Commun.*, 1969, **7**, 701–704.
2. Smolenskii, G. A., Isupov, V. A., Agranovskaya, A. I. and Krainik, N. N., New ferroelectrics of complex composition. *Sov. Phys. Solid State*, 1961, **2**, 2651–2654.
3. Smolenskii, G. A., Yudin, V. M., Sher, E. S. and Stolypin, Y. E., Antiferromagnetic properties of some perovskites. *Sov. Phys. JETP*, 1963, **16**, 622–624.
4. Moreau, J. M., Michel, C., Gerson, R. and James, W. J., Ferroelectric $BiFeO_3$ X-ray and neutron diffraction study. *J. Phys. Chem. Solids*, 1971, **32**, 1315–1320.
5. Ederer, C. and Spaldin, N. A., Weak ferromagnetism and magnetoelectric coupling in bismuth ferrite. *Phys. Rev. B*, 2005, **71**, 060401.
6. Sosnowska, I., Neumaier, T. P. and Steichele, E., Spiral magnetic ordering in bismuth ferrite. *J. Phys. C: Solid State Phys.*, 1982, **15**, 4835–4846.
7. Park, T.-J., Papaefthymiou, G. C., Viescas, A. J., Moodenbough, A. R. and Wong, S. S., Size-dependent magnetic properties of single-crystalline multiferroic $BiFeO_3$ powders. *Nano Lett.*, 2007, **7**, 766–772.
8. Mazumder, R., Sujatha Devi, P., Bhattacharya Dipten, Choudhury, P. and Sen, A., Ferromagnetism in nanoscale $BiFeO_3$. *Appl. Phys. Lett.*, 2007, **91**, 062510.
9. Carvalho, T. T. and Tavares, P. B., Synthesis and thermodynamic stability of multiferroic $BiFeO_3$. *Mater. Lett.*, 2008, **62**, 3984–3986.
10. Mukherjee, J. L. and Wang, F. F. Y., Kinetics of solid-state reaction of Bi_2O_3 and Fe_2O_3. *J. Am. Ceram. Soc.*, 1971, **54**, 31–34.
11. Kim, J. K., Kim, S. S. and Kim, W.-J., Sol–gel synthesis and properties of multiferroic $BiFeO_3$. *Mater. Lett.*, 2005, **59**, 4006–4009.
12. Chen, J.-C. and Wua, J.-M., Dielectric properties and Ac conductivities of dense single-phased $BiFeO_3$ ceramics. *Appl. Phys. Lett.*, 2007, **91**, 182903.
13. Lu, X. M., Xie, J. M., Song, Y. Z. and Lin, J. M., Surfactant-assisted hydrothermal preparation of submicrometer-sized two-dimensional $BiFeO_3$ plates and their photocatalytic activity. *J. Mater. Sci.*, 2007, **42**, 6824–6827.
14. Freitas, V. F., Grande, H. L. C., de Medeiros, S. N., Santos, I. A., Cótica, L. F. and Coelho, A. A., Structural, microstructural and magnetic investigations in high-energy ball milled $BiFeO_3$ and $Bi_{0.95}Eu_{0.05}FeO_3$ powders. *J. Alloys Compd.*, 2008, **461**, 48–52.
15. Szafraniak, I., Polomska, M., Hilczer, B., Pietraszko, A. and Kępiński, L., Characterization of $BiFeO_3$ nanopowder obtained by mechanochemical synthesis. *J. Eur. Ceram. Soc.*, 2007, **27**, 4399–4402.
16. Zhu, W. M. and Ye, Z.-G., Effects of chemical modification on the electrical properties of $0.67BiFeO_3$–$0.33PbTiO_3$ ferroelectric ceramics. *Ceram. Int.*, 2004, **30**, 1435–1442.
17. Buscaglia, M. T., Mitoseriu, L., Buscaglia, V., Pallecchi, I., Viviani, M., Nanni, P. and Siri, A. S., Preparation and charaterization of the manetoelectric $x BiFeO_3$–$(1-x)BaTiO_3$ ceramics. *J. Eur. Ceram. Soc.*, 2006, **26**, 3027–3030.
18. Srinivas, A., Boey, F., Sritharan, T., Kim, D. W., Hong, K. S. and Suryanarayana, S. V., Study of piezoelectric, magnetic and magnetoelectric measurements on $SrBi_3Nb_2FeO_{12}$. *Ceram. Int.*, 2004, **30**, 1431–1433.
19. Xu, J.-H., Ke, H., Jia, D.-C., Wang, W. and Zhou, Y., Low-temperature synthesis of $BiFeO_3$ nanopowders via a sol–gel method. *J. Alloys Compd.*, 2009, **472**, 473–477.
20. Dormann, J. L. and Nogues, M., Magnetic structures in substituted ferrites. *J. Phys.: Condens. Matter*, 1990, **2**, 1233–1237.
21. Zhang, S. T., Lu, M. H., Wu, D., Chen, Y. F. and Ming, N. B., Larger polarization and weak ferromagnetism in quenched $BiFeO_3$ ceramics with a distorted rhombohedral crystal structure. *Appl. Phys. Lett.*, 2005, **87**, 262907.
22. Pradhan, A. K., Zhang, K., Hunter, D., Dadson, J. B., Loutts, G. B., Bhattacharya, P., Katiyar, R., Zhang, J. and Sellmyer, D. J., Magnetic and electrical properties of single-phase multiferroic $BiFeO_3$. *J. Appl. Phys.*, 2005, **97**, 093903.
23. Krainik, N. N., Khuchua, N. P., Zhanova, V. V. and Evseev, V. A., Phase transitions in $BiFeO_3$. *Sov. Phys. Solid State*, 1966, **8**, 654–658.
24. Chen, C., Cheng, J. R., Yu, S. W., Che, L. J. and Meng, Z. Y., Hydrothermal synthesis of perovskite bismuth ferrite crystallites. *J. Cryst. Growth*, 2006, **291**, 135–139.